

Estimating statistical distributions using an integral identity

Cheng Zhang[†] & Jianpeng Ma^{†,‡,§}

[†]*Applied Physics Program &
Department of Bioengineering
Rice University*

Houston, TX 77005

[‡]*Verna and Marrs McLean Department of Biochemistry and Molecular Biology*

Baylor College of Medicine

One Baylor Plaza, BCM-125

Houston, TX 77030

[§] Email: jpma@bcm.tmc.edu

Abstract

We present an identity that provides an unbiased estimate of a general statistical distribution. The identity computes the distribution density from dividing a histogram sum over a local window by a correction factor from a mean-force integral. We show that the mean force can be evaluated as a configuration average, and the optimal window size is roughly the inverse of the local mean-force fluctuation. The new identity offers a more robust and precise estimate than a previous work by Adib and Jarzynski [J. Chem. Phys. (122): 14114, 2005]. It also allows a straightforward generalization to an arbitrary ensemble and a joint distribution of multiple variables. Particularly we derive a mean-force enhanced version of the weighted histogram analysis method (WHAM). The method can be used to improve distributions computed from molecular simulations. We illustrate the use in computing a potential energy distribution, a volume distribution in a constant pressure ensemble, a radial distribution function and a joint distribution of amino acid backbone dihedral angles.

I. Introduction

In the study, we present a method for estimating a general statistical distribution from data collected in a molecular simulation. The method is superior to the common approach of using a normalized histogram, which suffers from either a large noise when the bin size is small or a systematic bias when the bin size is large.

Our identity is akin to a previous one derived by Adib and Jarzynski¹ (hence the AJ identity), whereby the distribution density $\rho(x)$ at a point x is estimated from the number of visits to a window surrounding x , plus a correction from integrating the derivative of $\rho(x)$. The AJ identity improves over the histogram-based approach not only by eliminating the systematic bias from binning but also by smoothing out the resulting distribution, as the window contains much more data points than a single bin. However, the identity is slightly inconvenient as it neither ensures a positive output, nor determines its optimal parameters.

Here we present a new identity in which we construct a proper correction factor and use it to *divide* the number of visits to a local window to reach an unbiased estimate, as schematically illustrated in Fig. 1(a). The new strategy not only guarantees a positive-definite distribution, but also offers a simple estimate of the optimal window size, as it separates the error contributions from both the histogram and the mean force. The new identity also allows straightforward extensions to an arbitrary ensemble and to a joint distribution of multiple variables.

We describe the new identity in section II, present a few numerical applications in section III, and conclude the article in section IV with a few discussions.

II. Methods

II.A Integral identity

We wish to find an expression for the distribution density $\rho(x)$ at a point $x = x^*$.

To do so, we first approximate $\rho(x^*)$ by a histogram sum over a local window (x_-, x_+)

enclosing $x = x^*$, and then apply a correction factor. Formally, we have

$$\rho(x^*) = \frac{\int_{x_-}^{x_+} \rho(x) dx}{\int_{x_-}^{x_+} \rho(x) / \rho(x^*) dx},$$

where the numerator $\int_{x_-}^{x_+} \rho(x) dx$ counts the fraction of x falling into the window (x_-, x_+) ,

and can thus be measured from the histogram sum over the window.

Next, we convert the denominator to an integral as

$$\begin{aligned} \int_{x_-}^{x_+} \rho(x) / \rho(x^*) dx &= \int_{x_-}^{x_+} \exp[\log \rho(x) - \log \rho(x^*)] dx \\ &= \int_{x_-}^{x_+} \exp\left(\int_{x^*}^x (\log \rho)'(y) dy\right) dx, \end{aligned}$$

where we have moved $\rho(x^*)$ into the integral in the first step, then express the logarithm of the ratio as an integral of the “mean force” $(\log \rho)'(y)$. Hence, we have

$$\rho(x^*) = \frac{\int_{x_-}^{x_+} \rho(x) dx}{\int_{x_-}^{x_+} \exp\left(\int_{x^*}^x (\log \rho)'(y) dy\right) dx}. \quad (1)$$

We refer to Eq. (1) as the *fractional identity* in the follows. Unlike in the AJ identity¹, here the correction is applied as a divisor instead of additively. Nevertheless, it can be derived as a near-optimal modification of the AJ identity, as shown in Appendix A.

II.B Mean force from direct averaging

The identity Eq. (1) requires a mean force $(\log \rho)'(x)$ in addition to a histogram. In the follows, we construct a conjugate force $f_x = f_x(\mathbf{r}^N, \mathbf{s})$, as a function of molecular coordinates \mathbf{r}^N and other ensemble variables \mathbf{s} , such that its ensemble average is equal to the required mean force. Thus, in a molecular simulation, we can compute f_x for each trajectory frame and use its average as the mean force.

We first express x as a function $x = X(\mathbf{r}^N, \mathbf{s})$ of both molecular coordinates \mathbf{r}^N and (optionally) some variables \mathbf{s} of the simulation ensemble, e.g., \mathbf{s} can be the volume in an isobaric ensemble, or the temperature in a tempering simulation^{2,3}.

The distribution density $\rho(x)$ can now be written as

$$\rho(x) = \int \delta(X(\mathbf{r}^N, \mathbf{s}) - x) w(\mathbf{r}^N, \mathbf{s}) d\mathbf{r}^N d\mathbf{s}, \quad (2)$$

where $\delta(\dots)$ is the Dirac δ -function, and $w(\mathbf{r}^N, \mathbf{s})$ is the ensemble weight for a configuration \mathbf{r}^N and parameters \mathbf{s} , e.g., $w(\mathbf{r}^N, \mathbf{s}) \propto \exp[-\beta U(\mathbf{r}^N)]$ in case of a canonical ensemble (with $U(\mathbf{r}^N)$ being the potential energy, β temperature).

We evaluate its derivative as

$$\rho'(x) = \int -\frac{\partial}{\partial X} \delta(X(\mathbf{r}^N, \mathbf{s}) - x) w(\mathbf{r}^N, \mathbf{s}) d\mathbf{r}^N d\mathbf{s},$$

where we have used $\partial \delta(X - x) / \partial x = -\partial \delta(X - x) / \partial X$.

We proceed by introducing a vector field $\mathbf{v} = \mathbf{v}(\mathbf{r}^N, \mathbf{s})$ that satisfies $\mathbf{v} \cdot \nabla X = 1$ as a projection vector. For any vector \mathbf{u} , the inner product $\mathbf{v} \cdot \mathbf{u}$ gives the amplitude of the projection of \mathbf{u} onto the gradient ∇X . A convenient choice of the projection vector \mathbf{v} is $\mathbf{v} = \nabla X / (\nabla X \cdot \nabla X)$ (more generally it could be constructed from an arbitrary vector field

\mathbf{Y} as $\mathbf{v} = \mathbf{Y}/(\nabla X \cdot \mathbf{Y})$, as long as $\nabla X \cdot \mathbf{Y} \neq 0$). For later convenience, we have defined \mathbf{v} and ∇ on the joint vector space spanned by both the coordinates \mathbf{r}^N and parameters \mathbf{s} .

To use the projection vector, we insert $\mathbf{v} \cdot \nabla X = 1$ into the integrand and recall that the δ -function depends on coordinates \mathbf{r}^N or parameters \mathbf{s} only through X . Thus, the product of ∇X and $(\partial/\partial X)$ can be replaced by a single gradient operator ∇ , and

$$\begin{aligned}\rho'(x) &= \int -\mathbf{v} \cdot \nabla \delta(X(\mathbf{r}^N, \mathbf{s}) - x) w(\mathbf{r}^N, \mathbf{s}) d\mathbf{r}^N d\mathbf{s} \\ &= \int \delta(X(\mathbf{r}^N, \mathbf{s}) - x) w(\mathbf{r}^N, \mathbf{s}) f_x d\mathbf{r}^N d\mathbf{s},\end{aligned}$$

where we have integrated by parts, shifted the ∇ to the rest of the integrand, and defined a conjugate force $f_x \equiv \nabla \cdot \mathbf{v} + \mathbf{v} \cdot \nabla \log w(\mathbf{r}^N, \mathbf{s})$. Using Eq. (2), we find the mean force $(\log \rho)'(x) = \rho'(x)/\rho(x)$ is the average of f_x

$$(\log \rho)'(x) = \langle f_x \rangle_x = \langle \nabla \cdot \mathbf{v} + \mathbf{v} \cdot \nabla \log w(\mathbf{r}^N, \mathbf{s}) \rangle_x. \quad (3)$$

where $\langle \dots \rangle_x$ denotes an configuration average under a fixed x . Note, the above derivation is analogous to that of the dynamic temperature by Rugh⁴. For a canonical ensemble, the second term $\mathbf{v} \cdot \nabla \log w$ is reduced to $-\beta \mathbf{v} \cdot \nabla U$, i.e., the amplitude of the projection of the molecular force to the gradient of X , which is in accordance with the meaning of the “mean force” of $\langle f_x \rangle$.

II.C Optimal window size

We now determine the two window boundaries x_- and x_+ in Eq. (1) such that they minimize the statistical error in $\rho(x^*)$.

We first note that the histogram and mean-force data contribute independently to the numerator and denominator, respectively. How much the two contribute is however controlled by the window size. The output is dominated by the histogram contribution (numerator) with a narrow window, but by the mean-force contribution (denominator) with a wide window. For a narrow window, the denominator is reduced to the window width, and thus the identity is approximately a histogram average. At the other extreme, if the window covers the entire domain of x , the numerator becomes a constant, and the distribution is determined entirely by the mean-force integral on the denominator, i.e.,

$\rho(x^*) = \exp\left[\int_{x^*}^{x^*} (\log \rho)'(x) dx\right]$ (the lower bound of the integral is determined by the normalization).

As we increase the window size, the error of the numerator decreases as more data points reduces uncertainty, but that of the denominator increases as the error in the mean-force integral accumulates. The sum reaches a minimum at the optimal window.

Quantitatively, the relative error of the numerator $\varepsilon(N)/N$ is $1/\sqrt{N}$, where $N = N(x_-, x_+)$ is the number of independent data points included in the window.

The relative error of the denominator D is harder to compute exactly and thus is estimated from an upper bound. First, since D is an integral of $\exp(\Delta \log \rho)$, the relative error of D must be less than the maximal relative error of $\exp(\Delta \log \rho)$, or equivalently, the maximal absolute error of $\Delta \log \rho$. Next, since $\Delta \log \rho$ itself is an integral of the mean force, i.e., $\Delta \log \rho(x) = \int_{x^*}^x \langle f_x \rangle(x') dx'$, the maximum is likely to occur at either window boundary $x = x_{\pm}$. In the discrete version, the integral becomes a sum over bins

as $\Delta \log \rho = \sum_i \langle f_x \rangle(x_i) \delta x$ with δx being the bin size. Its error $[\varepsilon(\Delta \log \rho)]^2$, assuming no correlation among mean force at different bins, is $\sum_i \sigma_f^2(x_i) \delta x^2 / \delta n(x_i)$, where $\sigma_f^2(x_i)$ is the variance of the conjugate force at x_i , and $\delta n(x_i)$ is the number of independent data points in the bin at x_i .

On reaching the optimal window, including one more bin from either edge would keep the combined error $(\varepsilon(N)/N)^2 + (\varepsilon(D)/D)^2$ constant, i.e.,

$$-\frac{\delta n(x_{\pm})}{N(x_{-}, x_{+})^2} + \frac{\sigma_f^2(x_{\pm})}{\delta n(x_{\pm})} \delta x^2 = 0.$$

The first term represents the decrease of error due to increased sample size, while the second represents the increase due to the mean-force integration. Thus

$$\frac{\delta n(x_{\pm})}{N(x_{-}, x_{+})} = \sigma_{f.}(x_{\pm}) \delta x.$$

For a relatively a window, we have $N \approx \delta n w / \delta x$, with w being the window width. If we further replacing $\sigma_f(x_{\pm})$ by a local mean $\bar{\sigma}_f$, then

$$w = \gamma / \bar{\sigma}_f, \tag{4}$$

where γ is a heuristic factor which should be 1.0 ideally. However, as we overly estimate the error of the denominator, Eq. (4) somehow underestimates the optimal window size. In practice, we found the optimal γ was $1 \sim 2$.

On using Eq. (4), we remind the reader that σ_f is the mean-force fluctuation at a fixed x , i.e., $\sigma_f^2(x) = \langle f^2 \rangle_x - \langle f \rangle_x^2$, and thus is evaluated at the bin located at x . After the

intra-bin calculation, the quantity can then be averaged over a local or global window to produce $\bar{\sigma}_f$.

If the mean-force fluctuation is very small, Eq. (4) suggests abandoning the histogram data and switching to a mean-force integration. On the other hand, if the mean-force has a very large variance, one should stick to the histogram. Thus the method is effective only if the mean-force fluctuation is small. An attempt to reduce the mean-force fluctuation is described in Appendix B, where we improve the mean force itself by using data of the second-order derivatives of the distribution.

II.D Extension to weighted histogram analysis method

We now extend Eq. (1) to a composite distribution, which is a combination of several distributions under different conditions. The composite distribution can result from different independent simulations or an extended ensemble simulation, such as a tempering simulation, i.e., simulated ² and parallel tempering ³. For concreteness, we shall assume the composite distribution result from canonical distributions under different temperatures β_i with i being its label. Hence, each individual distribution is $\rho(x, \beta_i)$.

The aim is to estimate the distribution $\rho(x, \beta)$ at β , which needs not to be one of the β_i 's. A standard routine for this is the multiple histogram method, also known as the weighted histogram analysis method (WHAM) ⁵. Here, we derive an improved version whereby mean force information is utilized to improve the method.

Similar to the derivation of Eq. (1), we start from

$$\rho(x^*, \beta) = \frac{\sum_i N_i \int_{x_-}^{x_+} \rho(x, \beta_i) dx}{\sum_i N_i \int_{x_-}^{x_+} \rho(x, \beta_i) / \rho(x^*, \beta) dx},$$

where N_i is the total number of independent data points from the simulation at the temperature β_i , and the sum is carried over different temperatures β_i . To proceed, we simultaneously multiple and divide $\rho(x^*, \beta_i)$ on the denominator,

$$\sum_i N_i \int_{x_-}^{x_+} \frac{\rho(x, \beta_i)}{\rho(x^*, \beta)} dx = \sum_i N_i \frac{\rho(x^*, \beta_i)}{\rho(x^*, \beta)} \int_{x_-}^{x_+} \frac{\rho(x, \beta_i)}{\rho(x^*, \beta_i)} dx,$$

where the x -independent ratio $\rho(x^*, \beta_i) / \rho(x^*, \beta)$ has been moved out of the integral, leaving the other ratio $\rho(x, \beta_i) / \rho(x^*, \beta_i)$ to be converted the mean force integral at a fixed β_i as usual,

$$\rho(x^*, \beta) = \frac{\sum_i N_i \int_{x_-}^{x_+} \rho(x, \beta_i) dx}{\sum_i \left(N_i \frac{\rho(x^*, \beta_i)}{\rho(x^*, \beta)} \int_{x_-}^{x_+} \exp\left[\int_{x^*}^x (\log \rho)'(y, \beta_i) dy\right] dx \right)}. \quad (5)$$

For example, in case of the potential energy U distribution in a canonical ensemble, we have $w(U, \beta) = \exp(-\beta U) / Z(\beta)$, with $Z(\beta)$ being the partition function,

$$\rho(U^*, \beta) = \frac{\sum_i N_i \int_{U_-}^{U_+} \rho(U, \beta_i) dU}{\sum_i \left(N_i \exp[-(\beta_i - \beta)U^*] \frac{Z(\beta)}{Z(\beta_i)} \int_{U_-}^{U_+} \exp\left[\int_{U^*}^U (\langle \nabla \cdot \mathbf{v} \rangle_{U'} - \beta_i) dU'\right] dU \right)}, \quad (6)$$

where $\mathbf{v} = \nabla U / \nabla U \cdot \nabla U$. The regular WHAM⁵ is recovered with an infinitesimal window $U_- = U_+ = U^*$. Generally, Eq. (5) improves the histogram method by using the mean force data, e.g., the dynamic temperature $\langle \nabla \cdot \mathbf{v} \rangle_{U'}$ here. Note $\langle \nabla \cdot \mathbf{v} \rangle_{U'}$ is not a function of the temperature β , and since any two configurations with the same potential

energy U' always carry the same weight under any temperature β , the data for $\langle \nabla \cdot \mathbf{v} \rangle_{U'}$ collected from different temperatures are identical and thus can be merged.

III. Applications

III.A Potential energy distribution

We first compute a potential energy distribution $\rho(U)$ in a canonical ensemble, in which $w(\mathbf{r}^N, \beta) = \exp[-\beta U(\mathbf{r}^N)]/Z(\beta)$ with $Z(\beta)$ being the partition function. According to Eq. (3), the mean force $(\log \rho)'(U)$ can be computed from averaging $f_U = \nabla \cdot \mathbf{v} - \beta$, where $\mathbf{v} \equiv \nabla U / (\nabla U \cdot \nabla U)$. Note the conjugate force f_U has a clear physical meaning as the difference between the dynamic temperature ^{4,6} $\langle \nabla \cdot \mathbf{v} \rangle$ and the simulation parameter β .

We performed a molecular dynamics (MD) simulation on a 256-particle Lennard-Jones system under a smoothly switched potential (see Appendix C, $r_s = 2.0$ and $r_c = 3.0$). The temperature $\beta = 1.0$, density $\rho = 0.8$, time step $\Delta t = 0.002$. Velocity rescaling was used as the thermostat ⁷ with a time step 0.01.

The test sample consisted of 10^4 data points picked out from a trajectory of 10^7 MD steps with an interval of every 1000 steps. All frames from the trajectory were used to construct a reference distribution for comparison. A histogram of bin size $\delta U = 0.1$ was used in data collection and analyses.

We first demonstrate the use of the fractional identity Eq. (1) with a fixed window size $\Delta U = 12.5$, a value determined from Eq. (4) ($\gamma = 1.0$). The mean force $(\log \rho)'(U)$ was computed from a single bin at U (in case of an empty bin, we symmetrically enlarged

it until the window contained at least one data point). As shown in Fig. 2(a), the resulting distribution was much smoother than the histogram. For comparison, we computed the result from the AJ identity with the same window size. Though the results are generally similar, the AJ identity sometimes yielded negative values at the two edges, while the fractional identity appeared to be more robust and closer to the reference.

To show the gain from the integral identity approach, we define a KS difference (as commonly used in the Kolmogorov-Smirnov (KS) test ⁸ for detecting the difference between two distributions) as $\Delta_{\text{KS}} = (\sqrt{N} + 0.11 + 0.12/\sqrt{N})\Delta_{\text{CDF}}$, where N is the sample size, and Δ_{CDF} is the maximal difference between the cumulative distribution function (CDF) $F(x) = \int_{-\infty}^x \rho(y) dy$ of the resulting distribution and that from the reference. The smaller the quantity is, the more accurate the test distribution is. As the measure is independent of the bin size, it mainly detects the systematic bias in the test distribution instead of the smoothness of distribution density. As the identity is not optimized for the CDF (but for the distribution density), the KS difference serves as a stringent test.

The KS differences, computed for the histogram, the fractional identity Eq. (1) and the AJ identity Eq. (7) are shown in Fig. 2(b). It is clear that that both identities rendered more accurate distributions than the histogram. We also show there was an optimal window size that minimized the error. However, for the fractional identity, the optimal window size $\Delta U \approx 20.0$ was greater than the value 12.5 given by Eq. (4). Thus, a factor $\gamma \approx 1.5$ was used in other examples. Recall the KS difference scales with \sqrt{N} , thus from Fig. 2(b) we estimated about 20-fold increase of efficiency of using data around the optimal window. We also notice that with a smaller window, the fractional

identity gave better estimates than the AJ identity. This was expected as that the fractional identity is the optimal modification of the AJ identity in this case (Appendix A). With a larger window, the errors from both identities grew rapidly due to the larger involvement of the mean force data. As the fractional identity quickly switched to a mean-force based integral with a large window, its growth was faster. The comparison shows that choosing the window size is crucial to the success of the integral identity, and an overly large window can be counterproductive.

We performed a similar comparison in terms of the entropic distance defined as $D(\rho \parallel \rho^{\text{ref}}) = \int_{-\infty}^{\infty} \log[\rho(y)/\rho^{\text{ref}}(y)] \rho(y) dy$ for two distributions $\rho(x)$ and $\rho^{\text{ref}}(x)$. For the AJ identity, in case $\rho(x) < 0$, zero was assumed. Unlike the KS difference, this quantity directly compares the distribution density. As shown in Fig. 2(c), the fractional identity consistently produced a small entropic distance than the AJ identity, suggesting an improved smoothness. Interestingly, the error of the entropic distance also has a minimal, which occurred at a similar location $\Delta U \approx 20.0$ to that from the KS difference.

We now demonstrate the mean force improved weighted histogram analysis method (WHAM) introduced in Sec. II.D. In this case, we performed additional simulations at two neighboring temperatures $T = 0.8$ and $T = 1.2$. The reweighted distributions to $T = 1.0$ from both the original WHAM and the improved version are shown in Fig. 2(d), and as expected, the latter is much smoother than the former.

We further note that the identity approach is ensemble-dependent because the mean force depends on the ensemble weight w . To illustrate the point, we simulated the same system using a regular molecular dynamics without a canonical thermostat, i.e., we targeted a microcanonical ensemble in which the total energy was kept as a constant. In

the ensemble, the weight for a configuration, after averaging out momentum components, is $w(\mathbf{r}^N) \propto \sqrt{K}^{N_f-2} = \sqrt{E_{\text{tot}} - U(\mathbf{r}^N)}^{N_f-2}$, where N_f is the number of degrees of freedom, and K , U and E_{tot} are the kinetic, potential and total energy, respectively. The conjugate force is accordingly $f_U^M = \nabla \cdot \mathbf{v} - \frac{\frac{1}{2}N_f - 1}{E_{\text{tot}} - U(\mathbf{r}^N)}$, where $N_f = 3N - 6$, and the constant reference temperature β in the canonical ensemble is changed to an energy-dependent term $(\frac{1}{2}N_f - 1)/[E_{\text{tot}} - U(\mathbf{r}^N)]$.

The microcanonical-ensemble simulation was similar to the canonical-ensemble one. During equilibration, the kinetic energy was scaled regularly to match $\bar{T} \approx 1.0$, and was kept as a constant afterwards ($E_{\text{tot}} = -932$). As shown in Fig. 2(d), the distributions and mean forces (lower inset) from the two ensembles differed considerably, whereas the dynamic temperature $\langle \nabla \cdot \mathbf{v} \rangle$ (upper inset) matched. This example shows the importance of applying the correct formula for the mean force.

III.B Volume distribution

In the second example, we compute a volume distribution $\rho(V)$ in an isothermal-isobaric (i.e., constant temperature and pressure) ensemble^{9,10}. Unlike the previous case, the volume V is not a function of system coordinates, but an additional variable in the ensemble weight $w(\mathbf{r}^N, V)$. Particularly, the volume V serves as a scaling factor that translates the reduced (0 to 1) coordinates \mathbf{R}_i to the actual ones as $\mathbf{r}_i = \sqrt[3]{V} \mathbf{R}_i$. In terms of reduced coordinates, the ensemble weight can be written as

$w(\{\mathbf{R}_i\}, V) d\mathbf{R}^N dV \propto \exp[-\beta U(\{\sqrt[3]{V}\mathbf{R}_i\}) - \beta p V] V^N d\mathbf{R}^N dV$, where β and p are the reciprocal temperature and pressure, respectively.

According to Eq. (3), the conjugate force f_V is reduced to $\partial \ln w / \partial V$ in this case (the vector field \mathbf{v} is the unit vector along the direction of the parameter V , and hence $\nabla \cdot \mathbf{v} = 0$, $\mathbf{v} \cdot \nabla = \partial / \partial V$). Thus, $f_V = N/V - \beta \mathbf{r} \cdot \nabla U / (3V) - \beta p = \beta [p_c(\mathbf{r}^N) - p]$, represents the difference between the instantaneous pressure $p_c(\mathbf{r}^N) \equiv (N + \beta \mathbf{r} \cdot \mathbf{F} / 3) / V$ and the simulation parameter p .

There is however a subtle distinction between the apparent volume distribution $\rho(V)$ defined above and the actual physical one $\hat{\rho}(V)$. The difference arises from the fact that the partition function $Z(\beta, V)$ in the canonical ensemble includes all configurations with a volume *no larger than*, instead of equal to, the volume V of the simulation box. The partition function for configurations with volume precisely being in $(V - dV, V)$ is given by $(\partial Z / \partial V) dV = \langle p_c \rangle_V Z dV$. Thus the actual volume distribution $\hat{\rho}(V)$ differs from $\rho(V)$ by a factor, i.e., $\hat{\rho}(V) \propto \langle p_c \rangle_V \rho(V)$. The reader is referred to Koper and Reiss¹⁰ for a lucid and more detailed discussion.

A direct simulation according to $\hat{\rho}(V)$ is however inconvenient, as it requires one to know $\langle p_c \rangle_V$ in advance. In the follows, we shall use $\rho(V)$ to populate configurations during simulation, but report the adjusted $\hat{\rho}(V)$ after applying the correction.

We performed an MD simulation on the 256 Lennard-Jones system using the switched potential (with $r_s = 2.5$ and $r_c = 3.5$). The temperature $T = 1.24$ and pressure $p = 0.115$ is around the critical point. Velocity rescaling was used as the thermostat⁷

with a time step 0.01. For the pressure control, Monte Carlo volume moves were tried every two MD steps with a maximal magnitude of $\pm 2.0\%$ of the side length of the box. The trajectory contained 10^7 steps with the time step $dt = 0.002$.

We constructed the test sample from picking one out of every 100 frames from the trajectory and collect them using a histogram of bin width $\delta V = 1.0$. Data from the entire trajectories was used to produce reference curves. Since the volume changed almost by an order of magnitude, and the mean force fluctuation $\sigma_f \propto 1/V$, a fixed window size was not suitable. Thus we applied Eq. (4) with σ_f estimated from a local window, and $\gamma = 1.5$ (heuristic value). To apply the correction, a smooth $\langle p_c \rangle_V$ was computed from a second integral identity, Eqs. (10) and (11), in Appendix B. The window size was similarly determined from the local σ_f but with $\gamma = 3.0$.

As shown in Fig. 3, the volume distribution $\hat{\rho}(V)$ from the fractional identity was smoother than the histogram although it still had some ruggedness. From the inset, we observe that the window size grows linearly with the volume V . This example also clearly illustrates the danger of using an overly large window. We show in Fig. 3 the distribution from a pure mean-force integration $\rho(V) = \exp\left[\int^V (\log \rho)'(V') dV'\right]$ (which is the limiting case of using an infinite window, also corrected to the corresponding $\hat{\rho}(V)$ in the figure) manifested a much larger deviation from the reference (the deviation was however not systematic, as it diminished with the sample size). Thus choosing a proper window is crucial to the success of the method.

III.C Radial distribution function

In the third application, we compute a radial distribution function $g(r)$. We note that $g(r)$ is normalized in such a way that $g(r) \rightarrow 1$ at a large distance r , and thus it relates to the actual distribution density $\rho(r)$ as $\rho(r) = g(r)4\pi r^2/V_m$, where $V_m = \pi V/6$ is the volume of the sphere that fills the assumingly cubic simulation box, and the factor $4\pi r^2 dr/V_m$ gives the total probability of finding another particle in a sphere (radius r and thickness dr) centered at the test particle, if all particles were non-interacting. Thus, we modify Eq. (1) to $g(r^*) = \int_{r_-}^{r_+} \rho(r) dr / \int_{r_-}^{r_+} (4\pi r^2/V_m) \exp[\int_{r^*}^r (\log g)'(y) dy] dr$.

In a canonical ensemble, where $w(\mathbf{r}) \propto \exp(-\beta U)$, the conjugate force of $g(r_{12})$ for a pair of particles 1 and 2 is $f_r = \frac{1}{2}\beta \mathbf{F}_{12} \cdot \hat{\mathbf{r}}_{12}$, where β is the reciprocal temperature, $\mathbf{F}_{12} = \mathbf{F}_1 - \mathbf{F}_2$ is the difference between the force exerted on particles 1 and 2, and $\hat{\mathbf{r}}_{12}$ is the unit displacement vector from particle 2 to particle 1. To derive the result, we apply Eq. (3) with a vector field $\mathbf{v}_i = \frac{1}{2}\hat{\mathbf{r}}_{12}(\delta_{1i} - \delta_{2i})$, and note that $\langle f_r \rangle_r$ here corresponds to $(\log g)'(r)$ instead of $(\log \rho)'(r)$, and thus the divergence $\nabla \cdot \mathbf{v}$ term is exactly cancelled by the derivative from the additional normalization factor, as $\frac{d}{dr} \log 4\pi r^2/V_m = \nabla \cdot \mathbf{v} = 2/r$.

We simulated the 256 Lennard-Jones system under two different temperatures $T_1 = 0.85$ and $T_2 = 0.4$, using the switched potential ($r_s = 2.5$ and $r_c = 3.5$). The density $\rho = 0.7$ in both cases. Velocity rescaling with time step 0.01 was used as the thermostat⁷. After 5×10^4 steps of equilibration, we simulated another 5×10^4 steps with a time step $dt = 0.002$. From the entire trajectory, we picked 5 frames (from every 10^4 steps) as the

test sample, and 500 frames (every 10^2 steps) as the reference. The bin size $\delta r = 0.002$ was used in data collection and analyses.

Since this example was also used in the original Adib-Jarzynski paper¹, it is instructive to make a direct comparison between the two identities. As shown in Figure 4, the fractional identity produced smooth distributions with good agreement with the respective references in both temperatures, despite a relatively small sample size. On the other hand, although the Adib-Jarzynski identity (Eq. (20) in the reference with $R_1 = 1.0$)¹ also produced smooth distributions, there were appreciable deviations (especially at the lower temperature $T_2 = 0.4$) from the reference. The deviations were again not systematic, as they diminished with the sample size. We note the large deviations from the AJ identity were similar to those observed in the previous example of the volume distribution when a mean force integration was used to produce the distribution. Thus they were likely due to an overly large window, as the entire range of r , from 0 to half of the box size, was used as the window by the AJ identity. The error was larger at a lower temperature because the mean force changed more drastically there (hence larger mean force fluctuation). By contrast, in the fractional identity case, smaller windows, $\Delta r = 0.14$ for $T_1 = 0.85$ and $\Delta r = 0.09$ for $T_2 = 0.4$ were used according to Eq. (4) ($\gamma = 1.5$), and thus the output was more robust. We also note that the optimal window size shrunk at the lower temperature. This trend is universal. Since f_x has a component $\beta \mathbf{v} \cdot \mathbf{F}$ in the canonical ensemble, as one increases β (or lowers the temperature), the fluctuation grows, and thus the window size shrinks. The example again illustrates the critical influence from the window size.

III.D Amino acid backbone dihedral angles

Finally, we compute a joint distribution $\rho(\varphi, \psi)$ of the two backbone dihedrals φ and ψ of a glycine dipeptide. Here φ and ψ are the C'-N-C $_{\alpha}$ -C and N-C $_{\alpha}$ -C-N' dihedral angles respectively. To apply the identity, it is necessary to generalize Eq. (1) to the two dimensional case

$$\rho(\varphi^*, \psi^*) = \frac{\int_{\psi_-}^{\psi_+} \int_{\phi_-}^{\phi_+} \rho(\varphi, \psi) d\phi d\psi}{\int_{\psi_-}^{\psi_+} \int_{\phi_-}^{\phi_+} \exp[\log \rho(\varphi, \psi) - \log \rho(\varphi^*, \psi^*)] d\phi d\psi}.$$

On the denominator, $\log \rho(\varphi, \psi)$ can still be computed from the two mean force components $\frac{\partial}{\partial \varphi} \log \rho(\varphi, \psi)$ and $\frac{\partial}{\partial \psi} \log \rho(\varphi, \psi)$, but not via a direct integration, as the calculation is an overdetermined one (i.e. one distribution but two derivatives). Instead, we constructed $\log \rho(\varphi, \psi)$ in such a way that its two partial derivatives matched the observed values with a minimal overall deviation, see Appendix D.

The mean force are computed as averages as $\frac{\partial}{\partial \varphi} \log \rho(\varphi, \psi) = \langle \beta \mathbf{u} \cdot \mathbf{F} \rangle_{\varphi, \psi}$ and $\frac{\partial}{\partial \psi} \log \rho(\varphi, \psi) = \langle \beta \mathbf{v} \cdot \mathbf{F} \rangle_{\varphi, \psi}$, in which β is the temperature, \mathbf{F} is the force, and the two vector fields $\mathbf{u} = \nabla \varphi / (\nabla \varphi \cdot \nabla \varphi)$, $\mathbf{v} = \nabla \psi / (\nabla \psi \cdot \nabla \psi)$. A caveat was that in computing \mathbf{u} and \mathbf{v} , we only included the gradient component from the 1, 4 atoms, i.e., atoms C' and C for $\nabla \varphi$, atoms N and N' for $\nabla \psi$. Thus the mean force formulas (as shown above) were free from both the cross correlation between the two mean forces and the two divergences $\nabla \cdot \mathbf{u}$ and $\nabla \cdot \mathbf{v}$.

We dissolved the glycine dipeptide in a $32 \times 32 \times 32 \text{ \AA}^3$ TIP3P¹¹ water box, and simulated 36 ns with a time step 1 femtosecond. All chemical bonds of the peptide were allowed to vibrate. A double precision GROMACS 4.5¹² was used as the simulating

engine, The velocity rescaling method ⁷, SETTLE ¹³, and particle meshed Ewald (PME) sum ¹⁴ were used for thermostat, constraints in water molecules and long range electrostatic interaction, respectively. Non-bonded interactions were cutoff at 7 Å and shifted to zero until 8 Å. The PME grid spacing was 12 Å. Dihedral data were collected every step using a 1°×1° bin.

Due to a relatively large mean force fluctuation, we were only able to use small 4°×4° windows for the fractional identity, according to Eq. (4) (however, in case the window was empty, we expanded the window symmetrically until it included at least one data point). In Fig. 5, we show that the distribution $\rho(\varphi, \psi)$ from the fractional identity improved the smoothness over that from the normalized histogram. Particularly, the barrier regions, e.g. $\varphi \approx 0^\circ$, $\psi \approx \pm 100^\circ$, were enhanced. Additionally the forbidden band at $\varphi \approx \pm 180^\circ$, where the histogram was simply missing, was now filled by small but finite numbers. On the other hand, peaks at the helical and extended conformations were well preserved.

IV. Conclusions and discussions

In conclusion, we presented an identity, Eqs. (1) and (3), for estimating a general statistical distribution from data collected in molecular simulations. Compared with the previous identity-based approach ^{1,15}, the new identity offers a more general applicability (to any variable x and any ensemble, easily extensible to higher dimensional distributions, etc.), and at the same time a more robust and precise output.

The general expression for the conjugate force f_x Eq. (3) is also simpler than the conventional one from $-\beta \partial U / \partial x = -\beta \nabla U \cdot \partial \mathbf{r}^N / \partial x$ ¹⁵ in that it avoids a usually complex

coordinate transformation in computing $\partial \mathbf{r}^N / \partial x$ by replacing it with a simple force projection $\beta \mathbf{v} \cdot \mathbf{F}$ plus a divergence $\nabla \cdot \mathbf{v}$. Thus, it is applicable, at least in principle, to an arbitrary $x = X(\mathbf{r}^N)$. Though the computation of the divergence adds certain computational complexity, it can often be simplified or even avoided with a careful choice of the vector field \mathbf{v} (as in the dihedral example).

We also showed that the window size should be carefully chosen to maximize the benefit from the identity. An overly wide window risks a large error from the mean-force integration, although it usually yields a smoother distribution.

Finally, we wish to distinguish the method from an explicit smoothing method¹⁶. The current method does not assume a smooth distribution, but only seeks an *exact* expression for the distribution density with a hopefully minimal error. Although the use of the mean force $(\log \rho)'$ implies a differentiable distribution density $\rho(x)$, the mean force itself can be as oscillatory as an apparent noise. It is therefore possible that with reasonable approximations, the method can be further improved by introducing elements of the explicit smoothing methods.

Acknowledgements

We thank Dr. Michael Deem for introducing us to the work of Adib and Jarzynski and for many encouraging and helpful discussions. We also thank Dr. Thomas Woolf, Dr. John Straub, Dr. Michael Shirts and Dr. Thomas Truskett for helpful comments and discussions. JM acknowledges support from National Institutes of Health (R01-GM067801), National Science Foundation (MCB-0818353), The Welch Foundation (Q-1512), the Welch Chemistry and Biology Collaborative Grant from John S. Dunn Gulf

Coast Consortium for Chemical Genomics and the Faculty Initiatives Fund from Rice University. This work was also supported by the Shared University Grid at Rice funded by NSF under Grant EIA-0216467.

Appendix A. Alternative derivation of the fractional identity

We first rephrase the work of Adib and Jarzynski as the follows. The presentation is given with respect to a general distribution, and thus formally differs from the original one¹, which focused on a radial distribution. Nevertheless, the basic features are similar.

Firstly, any function $\rho(x)$ at $x = x^*$ can be evaluated as an integral over a window (x_-, x^*) as

$$\begin{aligned}\rho(x^*) &= \rho(x^*) \phi(x^*) - \rho(x_-) \phi(x_-) \\ &= \int_{x_-}^{x^*} [\rho(x) \phi'(x) + \rho'(x) \phi(x)] dx,\end{aligned}$$

where $\phi(x)$ is an arbitrary function under two conditions, $\phi(x_-) = 0$ and $\phi(x^*) = 1$; on the second line, the difference is converted to an integral within the range.

The range of integration can be enlarged to a window (x_-, x_+) that encloses x^* by applying the above equation to two windows (x_-, x^*) and (x^*, x_+) , $(x_- < x^* < x_+)$ with different $\phi(x)$'s, and then linearly combining them, see Fig. 1(b),

$$\rho(x^*) = \int_{x_-}^{x_+} [\rho(x) \phi'(x) + \rho'(x) \phi(x)] dx, \quad (7)$$

where the combined $\phi(x)$ satisfies

$$\begin{cases} \phi(x_+) = \phi(x_-) = 0, \\ \phi(x^{*-}) - \phi(x^{*+}) = 1, \end{cases} \quad (8)$$

with $\phi(x^{*-})$ and $\phi(x^{*+})$, the value of $\phi(x)$ immediately at the left and right of x^* respectively, serving as coefficients of combining the two windows. The function $\phi(x)$ is equivalent to the vector field $\mathbf{u}(\mathbf{r})$ in the original paper¹.

The problem of Eq. (7) is that it does not always yield a positive output since the correction in $\rho'(x)$ is free to overthrow the histogram contribution by random error.

We now derive the fractional identity Eq. (1) from Eq. (7). We start from a simple observation: if $f(x)$ is a function that equals to unity at $x = x^*$, i.e., $f(x^*) = 1$, then Eq. (7) applies not only to $\rho(x)$ itself, but also to the product $\rho(x)f(x)$, i.e.,

$$\rho(x^*) = \int_{x_-}^{x_+} [\rho(x)f(x)] \phi'(x) dx + \int_{x_-}^{x_+} [\rho(x)f(x)]' \phi(x) dx.$$

An arbitrary $f(x)$, or equivalently a reference distribution^{1,15}, does not guarantee a non-negative output. However, if we choose $f(x)$ such that $\rho(x)f(x)$ a constant, the second term on the right hand side of the above equation vanishes, and

$$\rho(x^*) = \int_{x_-}^{x_+} [\rho(x)f(x)] \phi'(x) dx. \quad (9)$$

Thus $\rho(x^*)$ is nonnegative as long as $\phi'(x)$ is so. The function $f(x)$ is obtained by integrating the distribution mean force from the boundary $f(x^*) = 1$ as

$$\begin{aligned} f(x) &= \exp \left\{ -[\log \rho(x) - \log \rho(x^*)] \right\} \\ &= \exp \left(- \int_{x^*}^x (\log \rho)'(y) dy \right). \end{aligned}$$

It is easily verified that $\frac{d}{dx} \log f(x) = -\frac{d}{dx} \log \rho(x)$ and hence $\frac{d}{dx} [\rho(x)f(x)] = 0$.

Finally, we determine $\phi(x)$ based on the observation that $\phi'(x)$ acts as a weight in Eq. (9). Thus, to minimize statistical error, $\phi'(x)$ should be inversely proportional to the variance of $\rho(x)f(x)$ ⁹. For a small window, we assume that the error of $\rho(x)f(x)$ comes mainly from the number of visits $\rho(x)$ instead of the modulation factor $f(x)$. Additionally, we assume the variance of $\rho(x)$ is proportional to $\rho(x)$, i.e., a Poisson distribution⁹, we thus have $\text{Var}[\rho(x)f(x)] = \text{Var}[\rho(x)] f^2(x) \propto \rho(x) f^2(x) \propto f(x)$.

$\phi'(x)$ can now be written as $C/f(x)$, where the constant C is determined from Eqs. (8) as

$$1 = \phi(x^{*-}) - \phi(x_-) + \phi(x_+) - \phi(x^{*+}) = \int_{x_-}^{x_+} \phi'(x) dx \quad (\text{the singularity at } x = x^* \text{ is ignored}).$$

Solving the equation gives $C = 1 / \int_{x_-}^{x_+} \exp\left(\int_{x^*}^x (\log \rho)'(y) dy\right) dx$, and Eq. (1) is recovered.

Appendix B. Improving the mean force

As suggested by Eq. (4), the optimal window size, hence the precision of the output from the integral identity Eq. (1), increases with the reduction of the mean force error. Hence, it is advantageous if one can improve the mean force $(\log \rho)'(y)$ itself. If the second-order derivative $(\log \rho)''(x)$ is available, one can apply an Adib-Jarzynski-like identity (see Appendix A):

$$(\log \rho)'(x_0) = \int_{x_-}^{x_+} [\varphi'(y) (\log \rho)'(y) + \varphi(y) (\log \rho)''(y)] dy, \quad (10)$$

where $\varphi(x)$ satisfies $\varphi(x_-) = \varphi(x_+) = 0$, $\varphi(x_0 - \delta) - \varphi(x_0 + \delta) = 1$. In practice, we use a linear function $\varphi(x) = (x - x_b)/(x_+ - x_-)$, with $x_b = x_-$ if $x < x_0$ or $x_b = x_+$ otherwise.

Note the window (x_-, x_+) can be different from that in Eq. (1). An averaging expression for computing $(\log \rho)''(x)$ can be found by taking the derivative of Eq. (3)

$$(\log \rho)''(x) = \left\langle (\Delta f_x)^2 \right\rangle_x + \left\langle \mathbf{v} \cdot \nabla f_x \right\rangle_x. \quad (11)$$

Eqs. (10) and (11) are particularly useful in computing the volume distribution, in which a smooth multiplicative correction term $\beta \langle p_c(V) \rangle_V$ can be obtained from the mean force $(\log \rho)'(V) = \beta (\langle p_c(V) \rangle_V - p)$ using the above method.

Appendix C. Switched Lennard-Jones potential

The Lennard-Jones potential is switched at $r = r_s$ to a polynomial $\sum_{k=4}^7 a_k (r - r_c)^k$ and extended to zero at $r = r_c$. For simplicity, we shall assume the reduced unit, where both the energy ε and radius σ units are 1.0. In our application in energy histograms, we need the potential and the first three derivatives to be continuous, since the derivative of the dynamic temperature requires up to the third-order derivative of the potential. The continuity at $r = r_c$ is guaranteed by the first four vanishing coefficients. To ensure the continuity up to third-order derivatives at $r = r_s$, the following parameters are used

$$\begin{aligned} a_4 &= 4 (35 r_s^3 A + 90 r_s^2 \Delta r B + 15 r_s \Delta r^2 C + 28 \Delta r^3 D) / (\Delta r^4 r_s^{15}), \\ a_5 &= -24 (14 r_s^3 A + 39 r_s^2 \Delta r B + 7 r_s \Delta r^2 C + 14 \Delta r^3 D) / (\Delta r^5 r_s^{15}), \\ a_6 &= 4 (70 r_s^3 A + 204 r_s^2 \Delta r B + 39 r_s \Delta r^2 C + 84 \Delta r^3 D) / (\Delta r^6 r_s^{15}), \\ a_7 &= -16 (5 r_s^3 A + 15 r_s^2 \Delta r B + 3 r_s \Delta r^2 C + 7 \Delta r^3 D) / (\Delta r^7 r_s^{15}), \end{aligned}$$

where, $\Delta r = r_c - r_s$, $A = 1 - r_s^6$, $B = 2 - r_s^6$, $C = 26 - 7r_s^6$, $D = 13 - 2r_s^6$.

Appendix D. Potential from the two-dimensional mean force

Unlike the one-dimensional case, determining a two-dimensional “potential” $u(x, y) \equiv \log \rho$ from the two mean force components $f_x = \partial u / \partial x$ and $f_y = \partial u / \partial y$ is an overdetermined problem, as the number of variables is only half of the number of the equations. Hence we seek a “best fit” solution in the follows.

We assume the potential is set up on a two-dimensional grid of $N \times M$ with a cell (bin) size $\delta x \times \delta y$. For a cell at (n, m) , where $n = 1, 2, \dots, N$, $m = 1, 2, \dots, M$, we wish to minimize the difference between the mean force value from $f_{n,m}$ and that from discretely

differentiating the u values at four cell corners $(u_{n+1,m} + u_{n+1,m+1} - u_{n,m} - u_{n,m+1})/(2\delta x)$ (and similarly for $g_{n,m}$). To the end, we minimize the following action S ,

$$S = \frac{1}{2} \sum_{n,m} \left[\left(\frac{u_{n+1,m} + u_{n+1,m+1} - u_{n,m} - u_{n,m+1}}{2} - f_{n,m} \delta x \right)^2 + \left(\frac{u_{n,m+1} + u_{n+1,m+1} - u_{n,m} - u_{n+1,m}}{2} - g_{n,m} \delta y \right)^2 \right].$$

At the minimum, we must have $\partial S / \partial u_{n,m} = 0$ for every $u_{n,m}$, i.e.,

$$u_{n,m} - \frac{u_{n-1,m-1} + u_{n-1,m+1} + u_{n+1,m-1} + u_{n+1,m+1}}{4} = \frac{f_{n-1,m-1} + f_{n-1,m} - f_{n,m-1} - f_{n,m}}{4} \delta x + \frac{g_{n-1,m-1} + g_{n,m-1} - g_{n-1,m} - g_{n,m}}{4} \delta y$$

The set of linear equations can be solved using Fourier transform. With

$\tilde{u}_{k,l} = \sum_{n,m} u_{n,m} \exp[-2\pi i (kn/N + lm/M)]$ ($\tilde{f}_{k,l}$ and $\tilde{g}_{k,l}$ similarly defined), we have

$$\tilde{u}_{k,l} = \frac{-i \exp \left[-\pi i \left(\frac{k}{N} + \frac{l}{M} \right) \right] \left[\sin \left(\frac{\pi k}{N} \right) \cos \left(\frac{\pi l}{M} \right) \tilde{f}_{k,l} \delta x + \cos \left(\frac{\pi k}{N} \right) \sin \left(\frac{\pi l}{M} \right) \tilde{g}_{k,l} \delta y \right]}{1 - \cos \left(\frac{2\pi k}{N} \right) \cos \left(\frac{2\pi l}{M} \right)}.$$

A final inverse Fourier transform yields the desired potential $u_{n,m}$ in the real space.

Figure Captions

Fig. 1 (a) The key of the fractional identity is to convert the ratio of a histogram sum (shaded area) to the distribution density $\rho(x^*)$ to an integral of the mean force. We then use the ratio to divide the observed histogram sum to obtain an unbiased estimate of $\rho(x^*)$. As both the histogram sum and ratio involves data from a window instead of a single bin, the resulting distribution is smoother due to the reduced uncertainty. **(b)** The auxiliary function $\phi(x)$ (solid) and its derivative $\phi'(x)$ (dashed, δ -function at $x = x^*$ excluded) employed by the Adib-Jarzynski identity (Appendix A).

Fig. 2 The potential energy distribution. **(a)** Comparison of the distributions from the histogram (gray), the fractional identity (Eq. (1), blue); and the Adib-Jarzynski (AJ) like identity (Eq. (7), red). **(b)** Error measured from the KS difference as a function of window size ΔU . **(c)** Error measured from the entropic distance. **(d)** The distribution from the weighted histogram analysis method (WHAM, red), compared with an improved version using the fractional identity (Eq. (6), blue). **(e)** Comparison of the distributions from a canonical ensemble (blue) and a microcanonical one (red).

Fig. 3 The volume distribution $\hat{\rho}(V)$ ($p = 0.115$ and $T = 1.24$, correction applied). Gray: the histogram; blue: the fractional identity; red: pure mean-force integration (limiting case with an infinite window). Inset: the window size.

Fig. 4 The radial distribution function $g(r)$. **(a)** $T_1 = 0.85$; **(b)** $T_2 = 0.4$. Gray: the histogram; blue: the fractional identity; red: the original Adib-Jarzynski (AJ) identity.

Fig. 5 The joint distribution of the two backbone dihedrals in the glycine dipeptide. **(a)**

The histogram; **(b)** the fractional identity.

References

- ¹ A. B. Adib and C. Jarzynski, J Chem Phys **122** (1), 14114 (2005).
- ² A. P. Lyubartsev, A. A. Martsinovski, S. V. Shevkunov, and P. N. Vorontsovvel'yaminov, Journal of Chemical Physics **96** (3), 1776 (1992); E. Marinari and G. Parisi, Europhysics Letters **19** (6), 451 (1992); C. Zhang and J. P. Ma, Physical Review E **76**, 036708 (2007).
- ³ R. H. Swendsen and J. S. Wang, Physical Review Letters **57** (21), 2607 (1986); C. J. Geyer, *Proceedings of the 23rd symposium on the interface* (American Statistical Association, New York, 1991); K. Hukushima and K. Nemoto, Journal of the Physical Society of Japan **65** (6), 1604 (1996); U. H. E. Hansmann, Chemical Physics Letters **281** (1-3), 140 (1997).
- ⁴ H. Rugh, Physical Review Letters **78**, 3 (1997).
- ⁵ A. M. Ferrenberg and R. H. Swendsen, Physical Review Letters **61** (23), 2635 (1988); A. M. Ferrenberg and R. H. Swendsen, Physical Review Letters **63** (12), 1195 (1989); J. D. Chodera, W. C. Swope, J. W. Pitera, C. Seok, and K. A. Dill, Journal of Chemical Theory and Computation **3** (1), 26 (2007); J. Kim, T. Keyes, and J. E. Straub, The Journal of Chemical Physics **135** (6), 061103.
- ⁶ B. D. Butler, G. Ayton, O. G. Jepps, and D. J. Evans, J Chem Phys **109** (16), 6519 (1998); O. G. Jepps, G. Ayton, and D. J. Evans, Phys Rev E Stat Phys Plasmas Fluids Relat Interdiscip Topics **62** (4 Pt A), 4757 (2000); Q. Yan and J. J. de Pablo, Phys Rev Lett **90** (3), 035701 (2003); C. Braga and K. P. Trivisa, J Chem

- Phys **123**, 134101 (2005); A. B. Adib, Phys Rev E Stat Nonlin Soft Matter Phys **71** (5 Pt 2), 056128 (2005).
- ⁷ G. Bussi, D. Donadio, and M. Parrinello, J. Chem. Phys. **126** (1), 014101 (2007).
- ⁸ W. H. Press, S. A. Teukolsky, W. T. Vetterling, and B. P. Flannery, *Numerical recipes in C: the art of scientific computing*, 2nd ed. (1992).
- ⁹ D. Frenkel and B. Smit, *Understanding Molecular Simulation From Algorithms to Applications*, Second ed. (Academic Press, 2002).
- ¹⁰ G. J. M. Koper and H. Reiss, The Journal of Physical Chemistry **100** (1), 422 (1996).
- ¹¹ W. L. Jorgensen, J. Chandrasekhar, J. D. Madura, R. W. I. Impey, and M. L. Klein, J. Chem. Phys. **79**, 926 (1983).
- ¹² D. Van Der Spoel, E. Lindahl, B. Hess, G. Groenhof, A. E. Mark, and H. J. Berendsen, J Comput Chem **26** (16), 1701 (2005).
- ¹³ S. Miyamoto and P. A. Kollman, J. Comput. Chem., 952 (1992).
- ¹⁴ U. Essman, L. Perela, M. L. Berkowitz, T. Darden, H. Lee, and L. G. Pedersen, J Chem Phys **103**, 16 (1995).
- ¹⁵ J. E. Basner and C. Jarzynski, J Phys Chem B **112** (40), 12722 (2008).
- ¹⁶ B. A. Berg and R. C. Harris, Computer Physics Communications **179**, 443 (2008); R. van Zon and J. Schofield, J Chem Phys **132** (15), 154110 (2010).

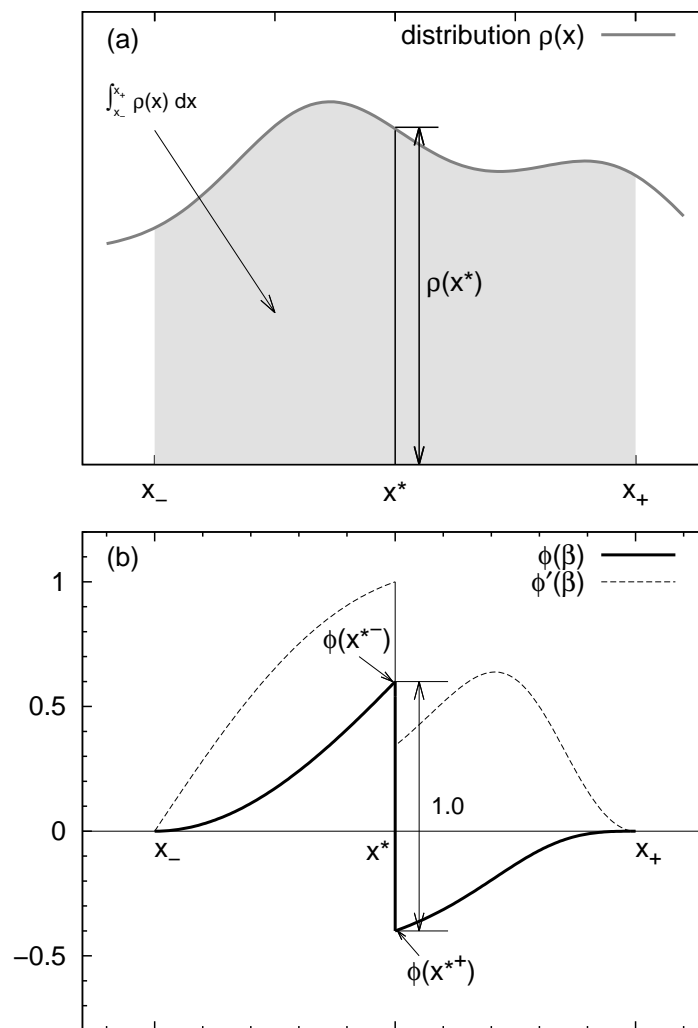
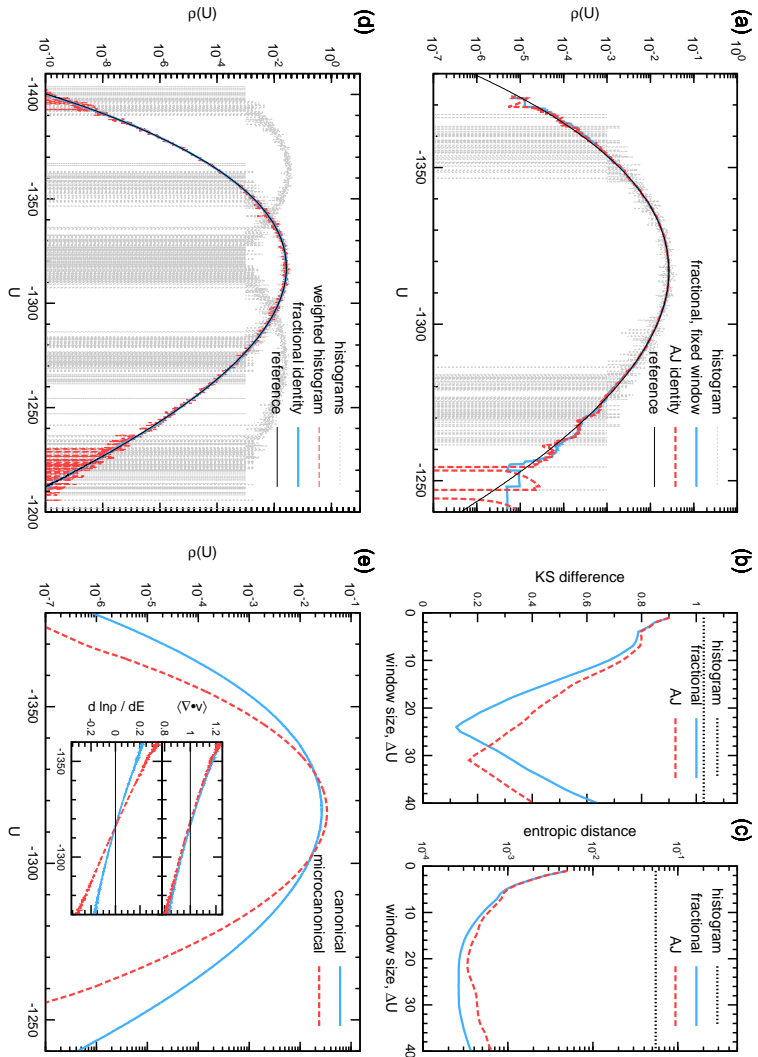
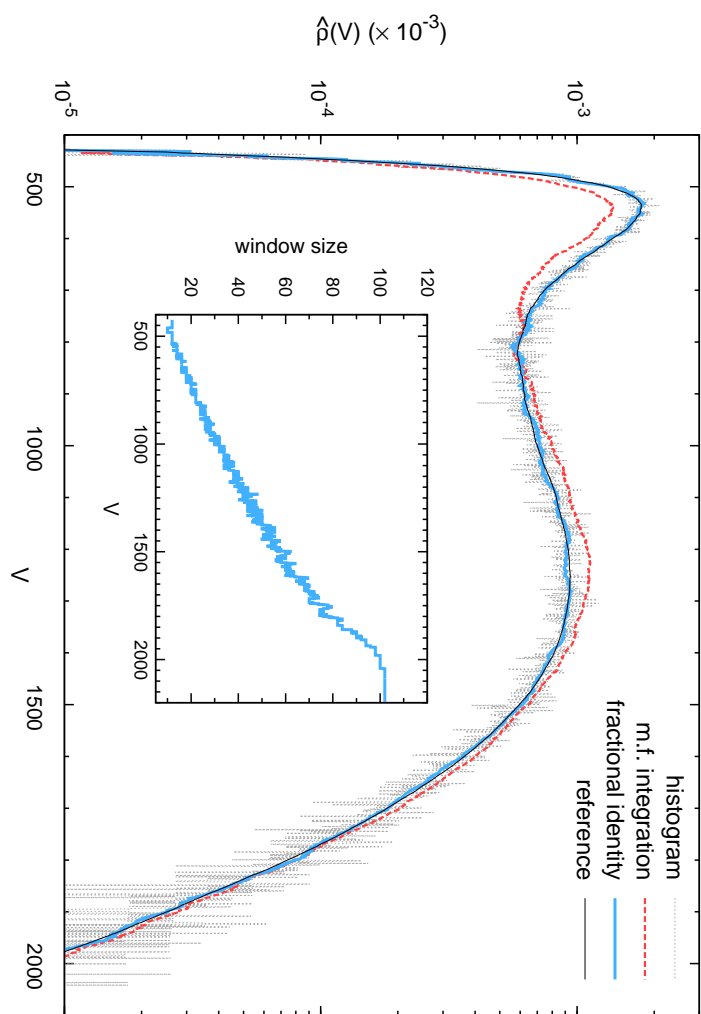
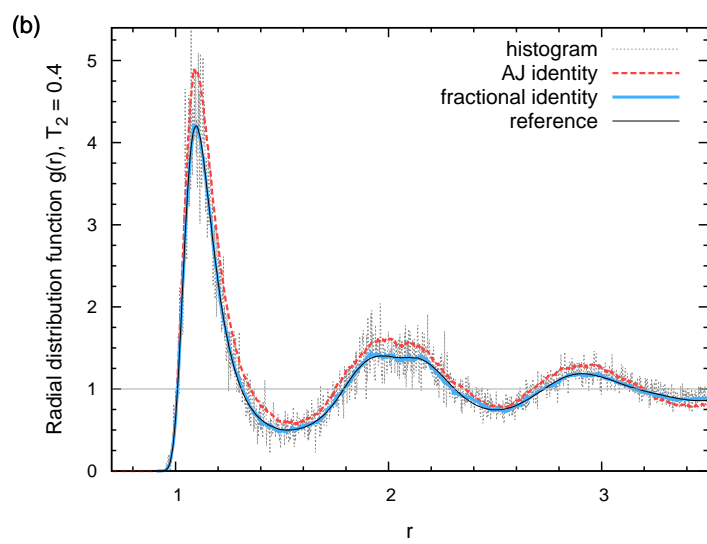
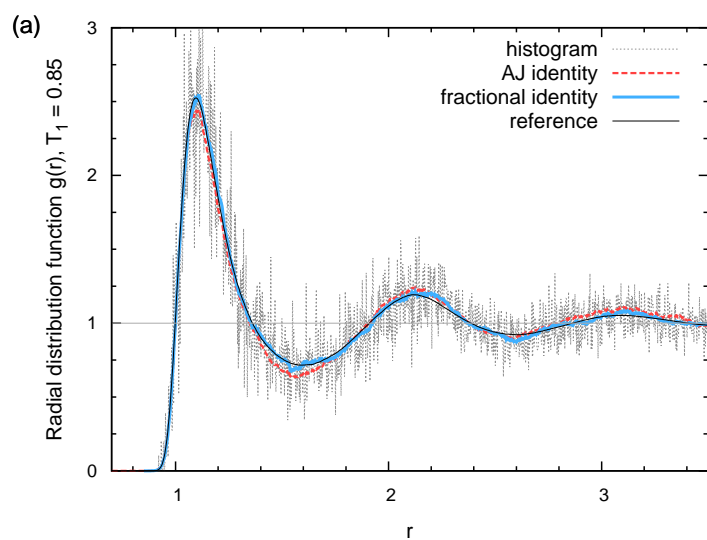


Figure 1:







$\log \rho(\phi, \psi)$

